Graph-based Observability Analysis of Bearing-only Cooperative Localization

Rajnikant Sharma, Randy Beard, Clark Taylor, and Stephen Quebe

***Abstract*—In this paper we investigate the nonlinear observability properties of bearing-only cooperative localization. We establish a link between observability and a graph representing measurements and communication between the robots. It is shown that graph theoretic properties like the connectivity and the existence of a path between two nodes can be used to explain the observability of the system. We obtain the maximum rank of the observability matrix without global information and derive conditions under which the maximum rank can be achieved. Furthermore, we show that for complete observability, all of the nodes in the graph must have a path to at least two different landmarks of known location.**

I. Introduction

In cooperative localization a group of robots exchange relative position measurements from their exteroceptive sensors (e.g., camera, laser, etc.) and their motion information (velocity and turn rate) from interoceptive sensors (e.g., IMU, encoders, etc.) to collectively estimate their states. Cooperative localization has been an active area of research (e.g., [1]–[8]) because it provides several potential advantages, including increased localization accuracy, sensor coverage, robustness, efficiency, and flexibility.

Recently, estimation algorithms such as the Extended Kalman Filter (EKF) [9], Minimum Mean Square Estimator (MMSE) [2], Maximum Likelihood Estimation (MLE) [10], Particle Filter [11], and Maximum A Posteriori (MAP) [12], have been used to solve the cooperative localization problem. These algorithms can be used either in a centralized [5] or decentralized manner [2], [9], [12]. For the localization errors to be bounded, it is required that the system be observable, independent of the estimation technique being used.

Several authors have carried out observability analysis of the cooperative localization problem. Initial results regarding the observability of cooperative localization were reported by Roumeliotis and Bekey [9]. They used linear observability analysis to show that the states of the robots performing cooperative localization are unobservable, but can be made observable by providing global positioning information to one of the robots. In [9] it was assumed that the absolute vehicle heading is measured directly and does not need to be estimated. Furthermore, linear approximation of a nonlinear system can provide different structural properties regarding the observability [13], [14]. Martinelli *et al*. [15] investigates the nonlinear observability of cooperative localization for two robots without heading measurements. They compared the observability properties of range and bearing measurements and showed that with either type of measurement, the maximum rank of the observability matrix is three, i.e., not fully observable. The analysis in [15] shows that relative bearing is the best observation between the robots. The part of the system which is observable is in general larger than for the other relative observations (relative distance and relative orientation). Accordingly, [15] uses polar coordinates for the observability analysis. Although polar coordinates simplify the analysis for two robots, we use a global coordinate system because it is more appropriate for graph level ($n > 2$) observability analysis.

In this paper, we extend the observability analysis presented in [15] from 2 to n robots, with bearing-only measurements. The extension for $n > 2$ is not obvious because of the dynamically changing set of $n(n-1)/2$ different relative bearing measurements leading to $2^{n(n-1)/2}$ possible configurations. Furthermore, since the robot states in [15] are not observable with respect to a global reference frame, and since it has been shown that two landmarks are needed for the observability of a single vehicle [16]–[18], in this paper we derive the number of landmarks needed for full observability of a group of n robots performing cooperative localization. In contrast to [9], we also assume that the heading of each robot is not directly measured but must be estimated.

To represent a group of robots, we will use the Relative Position Measurement Graph (RPMG) introduced in [19]. The nodes of an RPMG represent vehicle states and the edges represent bearing measurements between nodes. We establish a relationship between the graph properties of the RPMG and the rank of the system observability matrix. We prove that for a connected RPMG, the observability matrix for a team of n robots, which has size $3n \times 3n$ will have rank $3(n-1)$. We also derive conditions under which landmarks observed by a subset of robots enable the system to become fully observable.

The paper is organized as follows. In Section II we describe bearing-only cooperative localization and formulate the problem. In Section III we perform the nonlinear observability analysis. In Section IV we give our conclusions.

II. Bearing-only Cooperative Localization

Consider n robots moving in a horizontal plane performing cooperative localization. We can write the equations of motion for the i^{th} robot as,

$$\dot{X}_i = g_i(X_i, u_i) \triangleq \begin{pmatrix} V_i \cos\psi_i \\ V_i \sin\psi_i \\ \omega_i \end{pmatrix}, \tag{1}$$

where $X_i = [x_i \;\; y_i \;\; \psi_i]^\top \in \mathbb{R}^3$ is the robot state, including robot location $(x_i,\; y_i)$ and robot heading ψ_i, and $u_i = [V_i, w_i]^\top$ is the control input vector. We assume that onboard introspective sensors (e.g., encoders) measure the linear speed V_i and angular speed ω_i of the robot. Without loss of generality, we assume that robots cannot move backward ($V_i \geq 0,\; i = 1 \cdots n$). Each vehicle has an exteroceptive sensor to measure relative bearing to other vehicles and known landmarks that are in the field-of-view of the sensor. Relative bearing from the i^{th} robot to the j^{th} robot or landmark can be written as,

$$\eta_{ij} = \tan^{-1}\left(\frac{y_j - y_i}{x_j - x_i}\right) - \psi_i. \tag{2}$$

For cooperative localization, each robot exchanges its local sensor measurements (velocity, turn rate, and bearing to landmarks and other robots) with their neighbors. Let N_i^M be the set of neighbors for which robot i can obtain bearing measurements, and let N_i^C be the set of neighbors with which robots i can communicate. In this paper, we assume that $N_i^M = N_i^C$ and we will therefore denote the set of neighbors as N_i. To represent the connection topology of the robots we use a relative position measurement graph (RPMG) [19] which is defined as follows.

Definition 1: An RPMG for n robots performing cooperative localization with l different known landmarks is a directed graph

This paper is cleared for public release (88 ABW-11-0203)

This work is funded by an Air Force Young Investigator Award (FA9550-07-1-0167).

Rajnikant Sharma and Stephen Quebe are students in the Department of Electrical and Computer Engineering, Brigham Young University, Provo, UT, 84602 USA e-mail: raj.drdo@gmail.com, squebe@gmail.com.

Randal W. Beard is Professor in the Department of Electrical and Computer Engineering, Brigham Young University, Provo, UT, 84602 USA e-mail: beard@ee.byu.edu.

Clark N. Taylor is with the Air Force Research Laboratory, USA e-mail: Clark.Taylor@wpafb.af.mil.

Report Documentation Page

Form Approved
OMB No. 0704-0188

1. REPORT DATE	2. REPORT TYPE	3. DATES COVERED
APR 2012		**00-00-2012 to 00-00-2011**

4. TITLE AND SUBTITLE	5a. CONTRACT NUMBER
Graph-based Observability Analysis of Bearing-only Cooperative Localization	5b. GRANT NUMBER
	5c. PROGRAM ELEMENT NUMBER
6. AUTHOR(S)	5d. PROJECT NUMBER
	5e. TASK NUMBER
	5f. WORK UNIT NUMBER
7. PERFORMING ORGANIZATION NAME(S) AND ADDRESS(ES) **Brigham Young University,Department of Electrical and Computer Engineering,Provo,UT,84602**	8. PERFORMING ORGANIZATION REPORT NUMBER
9. SPONSORING/MONITORING AGENCY NAME(S) AND ADDRESS(ES)	10. SPONSOR/MONITOR'S ACRONYM(S)
	11. SPONSOR/MONITOR'S REPORT NUMBER(S)

12. DISTRIBUTION/AVAILABILITY STATEMENT
Approved for public release; distribution unlimited

13. SUPPLEMENTARY NOTES
IEEE Transactions on Robotics, Vol. 28, No. 2, p. 522-529, April, 2012. U.S. Government or Federal Rights License

14. ABSTRACT
In this paper we investigate the nonlinear observability properties of bearing-only cooperative localization. We establish a link between observability and a graph representing measurements and communication between the robots. It is shown that graph theoretic properties like the connectivity and the existence of a path between two nodes can be used to explain the observability of the system. We obtain the maximum rank of the observability matrix without global information and derive conditions under which the maximum rank can be achieved. Furthermore, we show that for complete observability, all of the nodes in the graph must have a path to at least two different landmarks of known location.

15. SUBJECT TERMS

16. SECURITY CLASSIFICATION OF:			17. LIMITATION OF ABSTRACT	18. NUMBER OF PAGES	19a. NAME OF RESPONSIBLE PERSON
a. REPORT **unclassified**	b. ABSTRACT **unclassified**	c. THIS PAGE **unclassified**	**Same as Report (SAR)**	**7**	

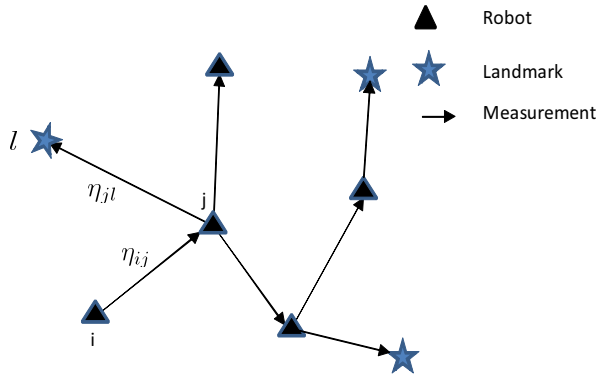

Fig. 1. Relative position measurement graph (RPMG). The nodes of an RPMG represent vehicle states and the edges represent bearing measurements between nodes.

$G_n^l \triangleq \{\mathcal{V}_{n,l}, \mathcal{E}_{n,l}\}$, where $\mathcal{V}_{n,l} = \{1, \cdots, n, n+1, \cdots, n+l\}$ is the node set consisting of n robot nodes and l landmark nodes and $\mathcal{E}_{n,l}(t) \subset \{\mathcal{V}_{n,0} \times \mathcal{V}_{n,l}\} = \{\eta_{ij}\}$, $i \in \{1, \cdots, n\}$, $j \in \{1, \cdots, n, n+1, \cdots, n+l\}$ is the edge set representing the availability of a relative bearing measurement. We use m to denote the number of edges in the RPMG. An example RPMG (G_5^3 with $m = 7$) is shown in Fig. 1.

Additionally, without loss of generality we assume that robots maintain a safe distance from each other and from landmarks, i.e., $R_{ij} > 0$, $\forall i, j = 1, \cdots n$ and landmarks $R_{ik} > 0$, $\forall i = 1, \cdots n$; $k = 1, \cdots, l$.

A. Lie Derivatives and Nonlinear Observability

To determine the observability of the entire system represented by the RPMG we use the nonlinear observability rank criteria developed by Hermann and Krener [20] which is summarized in the next paragraph.

Consider a system model with the following form

$$\Sigma: \begin{array}{c} \dot{X} = g(X,u) = [g_1^\top(X_1, u_1), \cdots, g_n^\top(X_n, u_n)]^\top \\ y = h(X,Z) = [h_1^\top(X,Z) \cdots h_m^\top(X,Z)]^\top \end{array} \quad (3)$$

where $X = [X_1^\top X_2^\top \cdots X_n^\top]^\top \in \mathbb{R}^{3n}$ is the state of the system, $Z = [Z_1^\top Z_2^\top \cdots Z_l^\top]^\top \in \mathbb{R}^{2l}$ is the position vector of all landmarks, $Z_i = [x_i \ y_i]^\top$ is the position vector of i^{th} landmark, $h_i : \mathbb{R}^{3n} \times \mathbb{R}^{2l} \mapsto \mathbb{R}$ is the measurement model of the i^{th} sensor, $u \in \Lambda \subseteq \mathbb{R}^{2n}$ is the control input vector, and $g : \mathbb{R}^{3n} \times \Lambda \mapsto \mathbb{R}^{3n}$. We consider the special case where the process function g can be separated into a summation of independent functions, each one excited by a different component of the control input vector, i.e.,

$$\dot{X} = g(X,u) = f_{v_1} V_1 + f_{\omega_1}\omega_1 + \cdots + f_{v_n} V_n + f_{\omega_n}\omega_n \quad (4)$$

The zeroth-order Lie derivative of any (scalar) function is the function itself, i.e., $L^0 h_k(X,Z) = h_k(X,Z)$. The first-order Lie derivative of function $h_k(X,Z)$ with respect to f_{v_i} is defined as

$$L^1_{f_{v_i}} h = \nabla L^0 h \cdot f_{v_i} \quad (5)$$

∇ represents the gradient operator, and $\cdot$ denotes the vector inner product. Considering that $L^1_{f_{v_i}} h_k(X,Z)$ is a scalar function itself, the second-order Lie derivative of $h_k(X,Z)$ with respect to f_{v_i} is

$$L^2_{f_{v_i} f_{v_i}} h = \nabla L^1_{f_{v_i}} h \cdot f_{v_i}. \quad (6)$$

Higher order Lie derivatives are computed similarly. Additionally, it is possible to define mixed Lie derivatives, i.e., with respect to different functions of the process model. For example, the second-order Lie derivative of h_k with respect to f_{v_j}, given its first derivative with respect to f_{v_i}, is

$$L^2_{f_{v_i} f_{v_j}} h = \nabla L^1_{f_{v_i}} h \cdot f_{v_j}. \quad (7)$$

Based on the preceding expressions for the Lie derivatives the observability matrix is defined as the matrix with rows

$$\mathcal{O} = \left\{ \nabla L^p_{f_{v_i}, \cdots, f_{v_j}, f_{\omega_i}, \cdots, f_{\omega_j}} h_k(X,Z) \right\} \quad (8)$$

where $i, j = 1, \cdots, n; k = 1, \cdots, m; p \in \mathbb{N}$. The important role of this matrix in the observability analysis of a nonlinear system is demonstrated by Theorem 1.

Theorem 1: A system is locally weakly observable if its observability matrix whose rows are given in (8) has full rank, e.g., in our case $rank(\mathcal{O}) = 3n$.

Additionally, we assume that the robot sensors have limited sensor range ρ_{sensor} and limited field of view. Therefore, agents can only measure the bearing of those robots and landmarks that are located within the footprint of the sensor. Therefore, the graph G_n^l will likely have a time varying topology.

III. Graph-based Observability Analysis

In this section, we obtain the conditions for the observability of the graph G_n^l. We derive explicit conditions that establish the rank of the observability matrix of the graph G_n^0 without landmarks, and the number of landmarks needed for the full rank of the observability matrix of the graph G_n^l.

A. Rows in the Observability matrix due to an Edge

In a graph G_n^l there are two types of edges: an edge between two robots, and an edge between a robot and a landmark. We derive the maximum number of linearly independent rows in the observability sub-matrix of an edge and the conditions for the maximum rank of the observability sub-matrix of an edge. The linearly independent rows of the observability sub-matrix of an edge serve as building block for the observability conditions for the graph G_n^l.

1) Edge between two robots: First we derive the linearly independent rows in the observability matrix for an edge η_{ij} between two robots and derive the conditions under which maximum number of linearly independent rows can be obtained.

We first find the Lie derivatives of η_{ij}. We rearrange the nonlinear kinematic equations in the following convenient form for computing Lie derivatives:

$$\dot{X} = \begin{bmatrix} \dot{X}_i \\ \dot{X}_j \end{bmatrix} = f_{v_i} V_i + f_{\omega_i}\omega_i + f_{v_j} V_j + f_{\omega_j}\omega_j \quad (9)$$

where $f_{v_i} = [c\psi_i \ s\psi_i \ 0 \ 0 \ 0 \ 0]^\top$, $f_{\omega_i} = [0 \ 0 \ 1 \ 0 \ 0 \ 0]^\top$, $f_{v_j} = [0 \ 0 \ 0 \ c\psi_j \ s\psi_j \ 0]^\top$, $f_{\omega_j} = [0 \ 0 \ 0 \ 0 \ 0 \ 1]^\top$, $c\psi_i \triangleq \cos\psi_i$, and $s\psi_i \triangleq \sin\psi_i$. We hereafter compute the necessary Lie derivatives of η_{ij} and their gradients.

Zeroth-order Lie derivative

$$L^0 h = \eta_{ij}$$

and gradient scaled by R_{ij}^2 is given by

$$\nabla L^0 h = \begin{bmatrix} -\Delta y_{ij} & \Delta x_{ij} & -R_{ij}^2 & \Delta y_{ij} & -\Delta x_{ij} & 0 \end{bmatrix}$$

where, $\Delta x_{ij} = x_i - x_j$,$\Delta y_{ij} = y_i - y_j$, and $R_{ij}^2 = (\Delta x_{ij})^2 + (\Delta y_{ij})^2$.

Remark 1: The scaling by R_{ij}^2 is an elementary row operation, therefore, it does not change the space spanned by the rows of the observability matrix. Also, it simplifies the computation of the higher order Lie derivatives.

First-order Lie derivatives

$$
\begin{aligned}
L^1_{f_{v_i}}h &= \nabla L^0 h \cdot f_{v_i} = \Delta x_{ij} s\psi_i - \Delta y_{ij} c\psi_i \\
L^1_{f_{v_j}}h &= \nabla L^0 h \cdot f_{v_j} = -(\Delta x_{ij} s\psi_j - \Delta y_{ij} c\psi_j) \\
L^1_{f_{\omega_i}}h &= \nabla L^0 h \cdot f_{\omega_i} = -R^2_{ij} \\
L^1_{f_{\omega_j}}h &= \nabla L^0 h \cdot f_{\omega_j} = 0
\end{aligned}
$$

with gradients given by

$$
\begin{aligned}
\nabla L^1_{f_{v_i}}h &= \begin{bmatrix} s\psi_i & -c\psi_i & J_i^+ & -s\psi_i & c\psi_i & 0 \end{bmatrix} \\
\nabla L^1_{f_{v_j}}h &= \begin{bmatrix} -s\psi_j & c\psi_j & 0 & s\psi_j & -c\psi_j & -J_j^+ \end{bmatrix} \\
\nabla L^1_{f_{\omega_i}}h &= 2\begin{bmatrix} -\Delta x_{ij} & -\Delta y_{ij} & 0 & \Delta x_{ij} & \Delta y_{ij} & 0 \end{bmatrix}
\end{aligned}
$$

where $J_i^+ = \Delta x_{ij} c\psi_i + \Delta y_{ij} s\psi_i$ and $J_j^+ = \Delta x_{ij} c\psi_j + \Delta y_{ij} s\psi_j$.

Second-order Lie derivatives

$$
\begin{aligned}
L^2_{f_{v_i}f_{v_i}}h &= \nabla L^1_{f_{v_i}}h \cdot f_{v_i} = s\psi_i c\psi_i - s\psi_i c\psi_i = 0 \\
L^2_{f_{v_j}f_{v_j}}h &= \nabla L^1_{f_{v_j}}h \cdot f_{v_j} = s\psi_j c\psi_j - s\psi_j c\psi_j = 0 \\
L^2_{f_{v_i}f_{v_j}}h &= \nabla L^1_{f_{v_i}}h \cdot f_{v_j} = -s\psi_i c\psi_j + s\psi_j c\psi_i \\
L^2_{f_{v_i}f_{\omega_i}}h &= \nabla L^1_{f_{v_i}}h \cdot f_{\omega_i} = J_i^+ \\
L^2_{f_{v_j}f_{\omega_j}}h &= \nabla L^1_{f_{v_j}}h \cdot f_{\omega_j} = -J_j^+ \\
L^2_{f_{\omega_i}f_{v_i}} &= \nabla L^1_{f_{\omega_i}}h \cdot f_{v_i} = -2J_i^+ \\
L^2_{f_{\omega_i}f_{v_j}} &= \nabla L^1_{f_{\omega_i}}h \cdot f_{v_j} = 2J_j^+
\end{aligned}
$$

with gradients given by

$$
\begin{aligned}
\nabla L^2_{f_{v_i}f_{v_j}}h &= \begin{bmatrix} 0 & 0 & -J_\psi & 0 & 0 & J_\psi \end{bmatrix} \\
\nabla L^2_{f_{v_i}f_{\omega_i}}h &= \begin{bmatrix} c\psi_i & s\psi_i & J_i^- & c\psi_i & s\psi_i & 0 \end{bmatrix} \\
\nabla L^2_{f_{v_j}f_{\omega_j}}h &= \begin{bmatrix} -c\psi_j & -s\psi_j & 0 & s\psi_j & -c\psi_j & -J_j^- \end{bmatrix}
\end{aligned}
$$

where $J_\psi = c\psi_i c\psi_j + s\psi_i s\psi_j$, $J_i^- = \Delta y_{ij} c\psi_i - \Delta x_{ij} s\psi_i$, and $J_j^- = \Delta y_{ij} c\psi_j - \Delta x_{ij} s\psi_j$.

Remark 2: Gradients of $L^2_{f_{\omega_i}f_{v_i}}$ and $L^2_{f_{\omega_i}f_{v_j}}$ are not included because they are linearly dependent on $\nabla L^2_{f_{v_i}f_{\omega_i}}h$ and $\nabla L^2_{f_{v_j}f_{\omega_j}}h$ respectively.

Third-order Lie derivatives

$$
\begin{aligned}
L^3_{f_{v_i}f_{v_j}f_{\omega_i}}h &= \nabla L^2_{f_{v_i}f_{v_j}}h \cdot f_{\omega_i} = -(c\psi_i c\psi_j + s\psi_i s\psi_j) \\
L^3_{f_{v_i}f_{v_j}f_{\omega_j}}h &= \nabla L^2_{f_{v_i}f_{v_j}}h \cdot f_{\omega_j} = (c\psi_i c\psi_j + s\psi_i s\psi_j) \\
L^3_{f_{v_i}f_{\omega_i}f_{v_i}}h &= \nabla L^2_{f_{v_i}f_{\omega_i}}h \cdot f_{v_i} = 1 \\
L^3_{f_{v_j}f_{\omega_j}f_{v_j}}h &= \nabla L^2_{f_{v_i}f_{\omega_j}}h \cdot f_{v_j} = 1 \\
L^3_{f_{v_i}f_{\omega_i}f_{\omega_i}}h &= \nabla L^2_{f_{v_i}f_{\omega_i}}h \cdot f_{\omega_i} = -(\Delta x_{ij} s\psi_i - \Delta y_{ij} c\psi_i) \\
L^3_{f_{v_j}f_{\omega_j}f_{\omega_j}}h &= \nabla L^2_{f_{v_i}f_{\omega_j}}h \cdot f_{\omega_j} = \Delta x_{ij} s\psi_j - \Delta y_{ij} c\psi_j
\end{aligned}
$$

with gradients given by

$$
\begin{aligned}
\nabla L^3_{f_{v_i}f_{v_j}f_{\omega_i}}h &= -\frac{\alpha}{\beta}\nabla L^2_{f_{v_i}f_{v_j}}h \\
\nabla L^3_{f_{v_i}f_{v_j}f_{\omega_j}}h &= \frac{\alpha}{\beta}\nabla L^2_{f_{v_i}f_{v_j}}h \\
\nabla L^3_{f_{v_i}f_{\omega_i}f_{\omega_i}}h &= -\nabla L^1_{f_{v_i}}h \\
\nabla L^3_{f_{v_j}f_{\omega_j}f_{\omega_j}}h &= -\nabla L^1_{f_{v_j}}h.
\end{aligned}
$$

where $\alpha = (s\psi_i c\psi_j - c\psi_i s\psi_j)$, and $\beta = c\psi_i c\psi_j + s\psi_i s\psi_j$.

Clearly, third and higher order Lie derivatives are linearly dependent on the gradients of second and lower order Lie derivatives. Therefore, with all the non-zero inputs the observability matrix of an edge between two robots can be written using gradients of Lie derivatives up to second-order as

$$
\mathcal{O}_{ij} = \begin{bmatrix}
-\Delta y_{ij} & \Delta x_{ij} & -R^2_{ij} & \Delta y_{ij} & -\Delta x_{ij} & 0 \\
s\psi_i & -c\psi_i & J_i^+ & -s\psi_i & c\psi_i & 0 \\
-s\psi_j & c\psi_j & 0 & s\psi_j & -c\psi_j & -J_j^+ \\
-2\Delta x_{ij} & -2\Delta y_{ij} & 0 & 2\Delta x_{ij} & 2\Delta y_{ij} & 0 \\
0 & 0 & -J_\psi & 0 & 0 & J_\psi \\
c\psi_i & s\psi_i & J_i^- & -c\psi_i & -s\psi_i & 0 \\
-c\psi_j & -s\psi_j & 0 & c\psi_j & s\psi_j & -J_j^-
\end{bmatrix}. \tag{10}
$$

Our objective is to find the number of linearly independent rows in $\mathcal{O}_{ij}$. Therefore, we transform $\mathcal{O}_{ij}$ into reduced row echelon form (RREF). RREF is the simplest possible form of a matrix, which directly provides the number of linearly independent rows in the matrix. Since RREF is the backbone of the analysis presented in this paper we state the next lemma, which explains the properties of a RREF matrix.

Lemma 1 ([21]): A matrix $A \in \mathbb{R}^{m\times n}$, by means of a finite sequence of elementary row operations, can be transformed to a row reduced echelon form $U \in \mathbb{R}^{m\times n}$ such that

$$EA = U \tag{11}$$

where $E \in \mathbb{R}^{m\times m}$ is the elementary operation matrix. If the rank of A is r then

1)
$$U = \begin{bmatrix} \mathbf{I}_r & B \\ \mathbf{0}_{(m-r)\times r} & \mathbf{0}_{(m-r)\times(n-r)} \end{bmatrix} \tag{12}$$
where $\mathbf{I}_r$ is the Identity matrix of size r and $B \in \mathbb{R}^{r\times(n-r)}$,
2) the first r rows of matrix U are linearly independent,
3) the non zero rows of the matrix U spans the same row space spanned by A,
4) if A is an invertible matrix ($r = m = n$) then U is the Identity matrix.

The next lemma provides conditions for the maximum rank of the observability matrix of an edge between two robots.

Lemma 2: The rank of $\mathcal{O}_{ij}$ given by (10) (edge between two robots) is three if

1) $V_i > 0$,
2) $V_j > 0$,
3) the i^{th} robot, which is measuring the bearing, does not move along the line joining the two robots,
4) the j^{th} robot does not move perpendicular to the line joining the two robots.

Proof: To prove the lemma, first we write J_i^- and J_j^+ as

$$J_i^- = v_1^\top v_i^{'} = \Delta y_{ij}\cos\psi_i - \Delta x_{ij}\sin\psi_i \tag{13}$$

$$J_j^+ = v_1^\top v_j = \Delta x_{ij}\cos\psi_j + \Delta y_{ij}\sin\psi_j \tag{14}$$

where $v_1 = [\Delta x_{ij}\ \Delta y_{ij}]^\top$ is a vector along the line between the two robots, $v_j = [\cos\psi_j\ \sin\psi_j]^\top$ is the heading vector of the j^{th} robot, and $v_i^{'} = [-\sin\psi_i\ \cos\psi_i]^\top$ is a vector perpendicular to the heading vector of the i^{th} robot.

From (13) and (14), we can verify that if the i^{th} robot, which is measuring the bearing, does not move along the line joining the two robots then $J_i^- \neq 0$, and if the j^{th} robot does not move perpendicular to the line joining the two robots then $J_j^+ \neq 0$. We then use the

elementary operation matrix

$$E_{ij} = \begin{bmatrix} -\frac{c\psi_j J_i^+}{J_i^- J_j^+} & -\frac{c\psi_j R_{ij}^2}{J_i^- J_j^+} & -\frac{\Delta y_{ij}}{J_j^+} & 0 & 0 & 0 & 0 \\ -\frac{s\psi_j J_i^+}{J_i^- J_j^+} & -\frac{s\psi_j R_{ij}^2}{J_i^- J_j^+} & \frac{\Delta x_{ij}}{J_j^+} & 0 & 0 & 0 & 0 \\ -\frac{s(\psi_j-\psi_i)}{J_i^- J_j^+} & \frac{J_j^-}{J_i^- J_j^+} & \frac{1}{J_j^+} & 0 & 0 & 0 & 0 \\ -\frac{2J_i^+}{J_i^-} & -\frac{2R_{ij}^2}{J_i^-} & 0 & 1 & 0 & 0 & 0 \\ \frac{1}{2}\frac{s(2\psi_i-2\psi_j)}{J_i^- J_j^+} & \frac{c(\psi_j-\psi_i)J_j^-}{J_i^- J_j^+} & \frac{c(\psi_i-\psi_j)}{J_j^+} & 0 & 1 & 0 & 0 \\ \frac{1}{J_i^-} & \frac{J_i^+}{J_i^-} & 0 & 0 & 0 & 1 & 0 \\ -\frac{J_i^+}{J_i^- J_j^+} & -\frac{R_{ij}^2}{J_i^- J_j^+} & -\frac{J_j^-}{J_j^+} & 0 & 0 & 0 & 1 \end{bmatrix}$$

which transforms O_{ij} as

$$E_{ij}\mathcal{O}_{ij} = U_{ij} = \begin{bmatrix} \mathbf{I}_3 & \bar{O}_{ij} \\ \mathbf{0}_{4\times 3} & \mathbf{0}_{4\times 3} \end{bmatrix} \tag{15}$$

where

$$\bar{O}^{ij} = \begin{bmatrix} -1 & 0 & \Delta y_{ij} \\ 0 & -1 & \Delta x_{ij} \\ 0 & 0 & -1 \end{bmatrix}. \tag{16}$$

From Lemma 1 we can say that RREF matrix U_{ij} has three linearly independent rows and these rows span the same observability space spanned by rows of $\mathcal{O}_{ij}$, therefore, maximum rank of $\mathcal{O}_{ij}$ is three. It should be noted that the top three non-zero rows in U_{ij} corresponds to L^0h, $L^1_{f_{v_i}}h$, and $L^1_{f_{v_j}}h$, therefore, conditions of the Lemma 2 are the sufficient conditions for $rank(\mathcal{O}_{ij}) = 3$. ■

2) Edge between a robot and a landmark: In this section, we derive the linearly independent rows in the observability matrix for an edge η_{ik} between a robot and a landmark and derive the conditions under which maximum number of linearly independent rows can be obtained. We rearrange the nonlinear kinematic equations in the following convenient form for computing Lie derivatives:

$$\dot{X}_i = f_{v_i}V_i + f_{\omega_i}\omega_i \tag{17}$$

where $f_{v_i} = [c\psi_i \; s\psi_i \; 0]^\top$ and $f_{\omega_i} = [0\; 0\; 1]^\top$. We hereafter compute the necessary Lie derivatives of η_{ik} and their gradients.

Zeroth-order Lie derivative

$$L^0h = \eta_{ik}$$

and its gradient, scaled by R_{ik}^2 is given by

$$\nabla L^0h = \begin{bmatrix} -\Delta y_{ik} & \Delta x_{ik} & -R_{ik}^2 \end{bmatrix}$$

where, $\Delta x_{ik} = x_i - x_k$, $\Delta y_{ik} = y_i - y_k$, and $R_{ik}^2 = (\Delta x_{ik})^2 + (\Delta y_{ik})^2$.

First-order Lie derivatives

$$L^1_{f_{v_i}} = \Delta x_{ik}s\psi_i - \Delta y_{ik}c\psi_i$$
$$L^1_{f_{\omega_i}} = -R_{ik}^2$$

with gradient given by

$$\nabla L^1_{f_{v_i}} = \begin{bmatrix} s\psi_i & -c\psi_i & \Delta x_{ik}c\psi_i + \Delta y_{ik}s\psi_i \end{bmatrix}$$
$$\nabla L^1_{f_{\omega_i}} = 2\begin{bmatrix} -\Delta x_{ik} & -\Delta y_{ik} & 0 \end{bmatrix}.$$

Second-order Lie derivatives

$$L^2_{f_{v_i}f_{v_i}}h = s\psi_i c\psi_i - s\psi_i c\psi_i = 0$$
$$L^2_{f_{v_i}f_{\omega_i}}h = \Delta x_{ik}c\psi_i + \Delta y_{ik}s\psi_i$$
$$L^2_{f_{\omega_i}f_{v_i}}h = -2L^2_{f_{v_i}f_{\omega_i}}h$$

with gradients given by

$$\nabla L^2_{f_{v_i}f_{\omega_i}}h = \begin{bmatrix} c\psi_i & s\psi_i & \Delta y_{ik}c\psi_i - \Delta x_{ik}s\psi_i \end{bmatrix}.$$

Remark 3: Gradient of $L^2_{f_{\omega_i}f_{v_i}}h$ is not included because it is linearly dependent on $\nabla L^2_{f_{v_i}f_{\omega_i}}h$.

Third-order Lie derivatives

$$L^3_{f_{v_i}f_{\omega_i}f_{v_i}} = 1$$
$$L^3_{f_{v_i}f_{\omega_i}f_{\omega_i}} = -(\Delta x_{ik}s\psi_i - \Delta y_{ik}c\psi_i) = -L^1_{f_{v_i}}.$$

Clearly, the gradients of third and higher order Lie derivatives are linearly dependent on the rows of the observability matrix corresponding to second and lower order Lie derivatives. Therefore, we can write the rows of the observability matrix corresponding to an edge between a robot and a landmark, using the gradients of Lie derivatives up to second order, as

$$\mathcal{O}_{ik} = \begin{bmatrix} -\Delta y_{ik} & \Delta x_{ik} & -R_{ik}^2 \\ s\psi_i & -c\psi_i & J^+ \\ -2\Delta x_{ik} & -2\Delta y_{ik} & 0 \\ c\psi_i & s\psi_i & J^- \end{bmatrix} \tag{18}$$

where $J^+ = \Delta x_{ik}c\psi_i + \Delta y_{ik}s\psi_i$ and $J^- = \Delta y_{ik}c\psi_i - \Delta x_{ik}s\psi_i$.

Lemma 3: The rank O_{ik} given by (18)(edge between a robot and a landmark) is two if

1) $V_i > 0$,
2) the robot does not move along the line joining the robot and the landmark.

Proof: If the robot does not move along the line joining the robot and the landmark then $J^- \neq 0$ and the elementary operation matrix

$$E_{ik} = \begin{bmatrix} \frac{-c\psi_i}{J^-} & \frac{-\Delta x_{il}}{J^-} & 0 & 0 \\ \frac{-s\psi_i}{J^-} & \frac{-\Delta y_{il}}{J^-} & 0 & 0 \\ \frac{-2J^+}{J^-} & \frac{-2R_{il}^2}{J^-} & 1 & 0 \\ \frac{1}{J^-} & \frac{J^+}{J^-} & 0 & 1 \end{bmatrix}$$

transforms O_{ik} as

$$E_{ik}\mathcal{O}_{ik} = U_{ik} = \begin{bmatrix} \bar{O}_{ik} \\ \mathbf{0}_{2\times 3} \end{bmatrix} \tag{19}$$

where

$$\bar{O}_{ik} = \begin{bmatrix} 1 & 0 & \Delta y_{ik} \\ 0 & 1 & -\Delta x_{ik} \end{bmatrix}. \tag{20}$$

It should be noted that the top two non-zero rows in the observability matrix are linearly independent (from Lemma 1) and they correspond to L^0h and $L^1_{f_{v_i}}$. Therefore, $V_i > 0$ and $J^- \neq 0$ are the sufficient conditions for the rank of the observability matrix being two. ■

Definition 2: An RPMG G_n^l (Definition 1) is called a proper RPMG if all the edges between robot nodes satisfy the conditions of Lemma 2 and all the edges between robots and landmarks satisfy Lemma 3.

In a proper RPMG each edge η_{ij} between two robots contribute three linearly independent rows to the observability matrix of a proper RPMG and each edge η_{ik} between a robot and a landmark contributes two linearly independent rows to the observability matrix of a proper RPMG. Using three linearly independent rows of U_{ij} in (15) and two linearly independent rows of U_{ik} in (19), we can write the observability matrix of a proper RPMG G_n^l as

$$O = \begin{Bmatrix} O_{ij} \\ O_{ik} \end{Bmatrix},\; i,j = 1,\cdots,n; k = 1,\cdots,l \tag{21}$$

where $O_{ij} = \begin{bmatrix} 0_{3\times 3(i-1)} & \mathbf{I}_3 & 0_{3\times(3(j-1)-3i)} & \bar{O}_{ij} & 0_{3\times 3(n-j)} \end{bmatrix}$ and $O_{ik} = \begin{bmatrix} 0_{2\times 3(i-1))} & \bar{O}_{ik} & 0_{2\times 3(n-i)} \end{bmatrix}$.

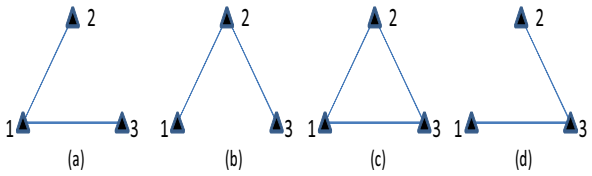

Fig. 2. The observability conditions between these four possible configurations of a connected, 3-node RPMG are identical.

Remark 4: The observability matrix O in (21) is not the original observability matrix of the graph G_n^l. Since the rows of (21) consist of the linearly independent rows after elementary row operations, from Lemma 1 we know that the rows of the observability matrix in (21) span the same observable space spanned by the original observability matrix.

B. Observability Analysis Without Landmarks

In this section we derive the conditions for achieving the maximum rank of the observability matrix for the graph G_n^0 without landmarks. We first discuss the observability properties for a 3-node graph G_3^0.

Lemma 4: If a three node proper RPMG G_3^0 is connected, then the rank of the observability matrix is six.

Proof: There are four possible configurations of a connected graph G_3^0, shown as sub-figures (a) through (d) in Fig. 2. We can write the transformed observability matrix for these configurations using (21) as

$$O_a = \begin{bmatrix} \mathbf{I}_3 & \bar{O}_{12} & \mathbf{0} \\ \mathbf{I}_3 & \mathbf{0} & \bar{O}_{13} \end{bmatrix} \quad O_b = \begin{bmatrix} \mathbf{I}_3 & \bar{O}_{12} & \mathbf{0} \\ \mathbf{0} & \mathbf{I}_3 & \bar{O}_{23} \end{bmatrix}$$
$$O_c = \begin{bmatrix} \mathbf{I}_3 & \bar{O}_{12} & \mathbf{0} \\ \mathbf{0} & \mathbf{I}_3 & \bar{O}_{23} \\ \mathbf{I}_3 & \mathbf{0} & \bar{O}_{13} \end{bmatrix} \quad O_d = \begin{bmatrix} \mathbf{I}_3 & \mathbf{0} & \bar{O}_{13} \\ \mathbf{0} & \mathbf{I}_3 & \bar{O}_{23} \end{bmatrix}.$$

We perform elementary operation on O_a, O_b, O_c, and O_d by multiplying them by elementary operation matrices $E_a = \begin{bmatrix} \mathbf{0}_3 & \mathbf{I}_3 \\ -\underline{O}_{12} & \underline{O}_{12} \end{bmatrix}$ where $\underline{O}_{12} = \begin{bmatrix} 1 & 0 & -\Delta y_{12} \\ 0 & 1 & \Delta x_{12} \\ 0 & 0 & 1 \end{bmatrix}$, $E_b = \begin{bmatrix} \mathbf{I}_3 & -\bar{O}_{12} \\ \mathbf{0}_3 & \mathbf{I}_3 \end{bmatrix}$, $E_c = \begin{bmatrix} \mathbf{I}_3 & -\bar{O}_{12} & \mathbf{0}_3 \\ \mathbf{0}_3 & \mathbf{I}_3 & \mathbf{0}_3 \\ -\mathbf{I}_3 & \bar{O}_{12} & \mathbf{I}_3 \end{bmatrix}$, and $E_d = \mathbf{I}_6$ respectively to get

$$E_a O_a = E_b O_b = E_d O_d = \begin{bmatrix} \mathbf{I}_3 & \mathbf{0} & \bar{O}_{13} \\ \mathbf{0} & \mathbf{I}_3 & \bar{O}_{23} \end{bmatrix},$$
$$E_c O_c = \begin{bmatrix} \mathbf{I}_3 & \mathbf{0} & \bar{O}_{13} \\ \mathbf{0} & \mathbf{I}_3 & \bar{O}_{23} \\ \mathbf{0} & \mathbf{0} & \mathbf{0} \end{bmatrix}.$$

Therefore, Lemma 1 implies that the observability sub-matrix of all the four configurations have six linearly independent rows and that these rows span the same observable space. ■

Remark 5: The elementary operation matrix E_d for observability matrix O_d in Lemma 4 is Identity because O_d is already in a reduced row echelon form.

From Lemma 4 we can say that the rows of two edges for a proper RPMG with a common node are independent. The following lemma is an extension of this idea.

Lemma 5: If a graph G_n^0 is a proper RPMG and has the form of a 2-level tree (see figure 3(f)) which consists of a root node and $n-1$ leafs directly connected to the root, then the rank of the associated observability matrix is $3(n-1)$.

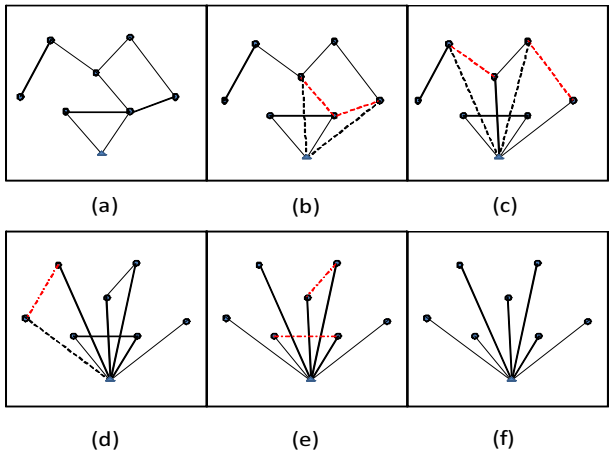

Fig. 3. An example of converting an arbitrary connected RPMG to a 2-level tree.

Proof: Without loss of generality, assume that the root node of the 2-level tree is labelled as n. The system observability matrix will then be of the form

$$O_{2-level} = \begin{bmatrix} \mathbf{I}_3 & \mathbf{0} & \mathbf{0} & \cdots & \bar{O}_{1n} \\ \mathbf{0} & \mathbf{I}_3 & \mathbf{0} & \cdots & \bar{O}_{2n} \\ \vdots & & \ddots & & \vdots \\ \mathbf{0} & \mathbf{0} & \cdots & \mathbf{I}_3 & \bar{O}_{n-1,n} \end{bmatrix} \tag{22}$$

Clearly, the rank is $3(n-1)$. ■

Theorem 2: If the graph G_n^0 is a proper connected RPMG then the rank of the associated observability matrix is $3(n-1)$.

Proof: Using Lemma 4, any connected 3-node subgraph in the larger graph can be replaced with any other connected 3-node subgraph, without affecting the rank of the system observability matrix because their associated observability sub-matrices span the same observable sub-space. A connected graph G_n^0 can be transformed to a 2-level tree using following algorithm.

1) Choose any node and label it as the root as shown in Fig. 3 (a).
2) Select the nodes whose path from the root consists of two edges(three nodes including root) as shown in Fig. 3 (b). Each such path can be represented as a 3-node subgraph G_3^0.
3) If a valid 3-node subgraph is found, perform a subgraph replacement (see Fig. 3 (c)) so that nodes j and i are both a distance of one away from the root node and repeat step 2. If a valid subgraph G_3^0 is not found, continue to step 4.
4) Search for a three node subgraph G_3^0 that includes the root node and two nodes (nodes j and i) distance one away from the root node that contain an edge between these two nodes (see Fig. 3 (d)).
5) If a valid 3-node subgraph was found, perform a subgraph replacement that maintains the edges between the root node and nodes i and j, but removes the edge between nodes i and j (see Fig. 3 (e)). Repeat step 4 until G_0^n is transformed into a 2-level tree.

To show that this algorithm transforms a connected proper RPMG to a 2-level tree, first consider steps 2 and 3. Every time step 2 finds a valid subgraph, the distance of node i to the root node will be decreased from two to one. Because the graph is connected, the root node will be connected to any other node within a finite number of steps. Therefore, as steps 2 and 3 continue to execute, all nodes will be brought to a maximum of distance one away from the root node. This is similar to the graph shown in Fig. 3(e). Steps 4 and 5 simply remove any redundant edges. Therefore, this algorithm converts any

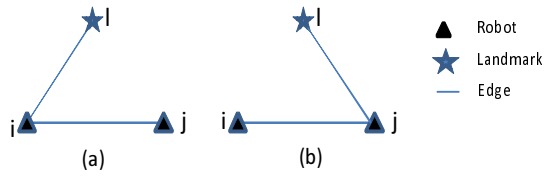

Fig. 4. Two robots and one landmark RPMG G_2^1.

connected graph to a 2-level tree. The algorithm is also a recursive way of performing elementary row operations on the rows of the observability matrices of sub-graphs G_3^0 to show that the observability matrix of the connected and proper RPMG G_n^0 is equivalent to the observability matrix of a 2-level tree. Furthermore, we can say that the basis of the observable space of a connected proper RPMG G_n^0 is the rows of $O_{2-level}$ and from Lemma 5, the rank of the observability matrix is $3(n-1)$. ■

C. Observability Analysis With Known Landmarks

In this subsection, we assume that landmarks of known location are observed by robots within the network, providing information about the global coordinate system. We derive conditions for complete observability of the graph G_n^l. First we derive the conditions for the observability of a single robot.

Lemma 6: The rank of the observability matrix of a proper RPMG G_1^l (one robot and l landmarks) is three if there are at least two landmarks ($l \geq 2$) and the robot and two landmarks are not on the same line (i.e., $\eta_{i1} \neq \eta_{i2}$).

Proof: Consider a proper RPMG G_1^2 with one vehicle and two landmarks such that $\eta_{i1} \neq \eta_{i2}$. Using (21) the observability matrix of graph G_1^2 can be written as, $O = \begin{bmatrix} \bar{O}_{i1} \\ \bar{O}_{i2} \end{bmatrix}$. To find the number of linearly independent rows we perform elementary row operations on O by multiplying by $E_{i12} = \begin{bmatrix} \frac{\Delta y_{i2}}{\Delta y_{12}} & 0 & -\frac{\Delta y_{i1}}{\Delta y_{12}} & 0 \\ -\frac{\Delta x_{i1}}{\Delta y_{12}} & 1 & \frac{\Delta x_{i1}}{\Delta y_{12}} & 0 \\ -\frac{1}{\Delta y_{12}} & 0 & \frac{1}{\Delta y_{12}} & 0 \\ -\frac{\Delta x_{12}}{\Delta y_{12}} & -1 & -\frac{\Delta x_{12}}{\Delta y_{12}} & 1 \end{bmatrix}$ to obtain

$$E_{i12}O = \begin{bmatrix} \mathbf{I}_3 \\ \mathbf{0}_{1\times 3} \end{bmatrix}.$$

This implies that two different landmarks provides three independent rows to the observability matrix. Therefore, from Theorem 1 the single robot states are completely observable, i.e., $rank(O) = 3$. ■

From Lemma 6 we know that, if all of the n vehicles in the group are directly connected to two different landmark, then the system is completely observable ($rank(O) = 3n$). However, due to limited sensor range and bearing all of the vehicles in the group may not be able to see two landmarks. The following lemmas and theorem show how cooperative localization can overcome constraints posed by sensor limitations.

Lemma 7: Given a 3-node RPMG G_2^1 with two robots and one landmark, if the graph G_2^1 is proper then the rows of the observability matrix of the two configurations of G_2^1 shown in Fig. 4(a) and Fig. 4(b) spans the same observable space.

Proof: The two configurations shown in Fig. 4(a) and Fig. 4(b) only differs in the landmark l connection. In configuration (a) the landmark is directly connected to the i^{th} node whereas in configuration (b) the landmark is directly connected to the j^{th} node. The observability matrix for the configurations shown in Fig. 4(a) and (b)

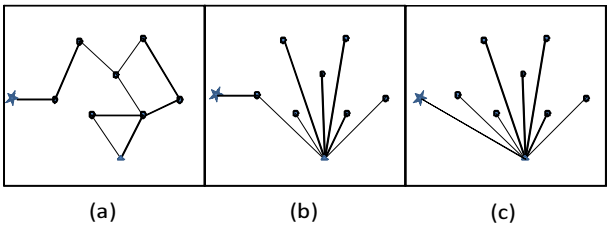

Fig. 5. An example of converting an arbitrary connected RPMG with landmark to a two-level tree.

can be written using (21) as

$$O_a = \begin{bmatrix} \mathbf{I}_3 & \bar{O}_{ij} \\ \bar{O}_{il} & 0_{2\times 3} \end{bmatrix}, \; O_b = \begin{bmatrix} \mathbf{I}_3 & \bar{O}_{ij} \\ 0_{2\times 3} & \bar{O}_{jl} \end{bmatrix}. \quad (23)$$

We can perform elementary operation on O_a by multiplying by the elementary operation matrix $E_{ijl} = \begin{bmatrix} \mathbf{I}_3 & \mathbf{0}_{3\times 2} \\ -\bar{O}_{il} & \mathbf{I}_2 \end{bmatrix}$ to show that $E_{ijl}O_a = O_b$. Therefore, from Lemma 1 we can say that the observability matrix of both the configurations spans the same space. ■

Lemma 8: Given the RPMG G_n^l , if it is proper and connected then the associated observability matrix is equivalent (observability matrix of both graphs span the same space) to the observability matrix of a 2-level tree.

Proof: Consider a connected proper RPMG G_n^l(example for $l = 1$ is shown in Fig. 5(a)). We can write the observability matrix for the graph G_n^l using (21). To show that the observability matrix of a connected proper RPMG G_n^l is equivalent (observability matrix of both graphs span the same space) to the observability matrix of a 2-level tree we perform following steps.

- First we perform elementary operations only on the rows of the observability matrix of the edges between robots (subgraph G_n^0). From Theorem 2 we know that these operations leads to the observability matrix of a 2-level tree. Therefore, the resulting observability matrix of the graph G_n^l is equivalent to the observability of the 3-level tree (Example shown in Fig 5(b)) with landmarks on level three. In the 3-level tree the path between each landmark and the root consists of two edges, including edge η_{ji} between the root and the i^{th} node (landmark is directly connected to i^{th} node) and edge η_{il} between landmark l and the i^{th} node. The path between each landmark and the root can be represented as a subgraph G_2^1 with two robots and one landmark. There are l such subgraphs in the graph G_n^l.
- Next we perform elementary operations on the rows of the observability matrix of each subgraph G_2^1 associated with each landmark. From Lemma 7 we know that the resulting observability matrix of the graph G_n^l is equivalent to the observability matrix of a two-level tree (see Fig. 5(c)) with $n-1$ robot-to-robot leafs and l leafs between root and landmarks.

■

Theorem 3: Given a proper RPMG G_n^l, if for each robot there exists a path to at least two landmarks and the robot and two landmarks are not on the same line (i.e., $\eta_{i1} \neq \eta_{i2}, \forall\, i = 1, \cdots, n$) then the system is completely observable, i.e., the rank of the observability matrix is $3n$.

Proof: There are two scenarios for paths between landmarks. (1) All the robots are directly connected to the landmarks. For this case, from Lemma 6 we know that the proper RPMG G_n^l is completely observable if $l \geq 2$ and $\eta_{i1} \neq \eta_{i2}, \forall\, i = 1, \cdots, n$. (2) Consider the general case where the proper RPMG G_n^l is connected and only a subset of nodes measure landmarks. In this case all of the robots are

not directly connected to landmarks, but there exists a path between each robot and the landmarks. From Lemma 8 we know that the observability matrix of a connected proper RPMG G_n^l is equivalent to the observability matrix of a 2-level tree. Therefore connected proper RPMG G_n^l can be replaced by a two-level tree with $n-1$ robot to robot leafs and l leafs between the root and landmarks. Furthermore, from Lemma 5 we know that for a 2-level tree all of the $3(n-1)$ rows of the observability matrix of $n-1$ edges between all robots are linearly independent. Therefore, we only consider a subgraph (two-level) G_2^2 which consists of three edges, including an edge η_{ij} between the root (j^{th} node) and i^{th} node and two edges η_{j1} and η_{j2} between the root and two landmarks. Using (21) the observability matrix for this sub-graph G_2^2 is given by

$$O = \begin{bmatrix} \mathbf{I}_3 & \bar{O}_{ij} \\ 0_{2\times 3} & \bar{O}_{j1} \\ 0_{2\times 3} & \bar{O}_{j2} \end{bmatrix} \tag{24}$$

We perform elementary operation on (24) using

$$E_{ij12} = \begin{bmatrix} 1 & 0 & 0 & \frac{\Delta y_{i2}}{\Delta y_{12}} & 0 & -\frac{\Delta y_{i1}}{\Delta y_{12}} & 0 \\ 0 & 1 & 0 & -\frac{\Delta x_{i1}}{\Delta y_{12}} & 1 & \frac{\Delta x_{i1}}{\Delta y_{12}} & 0 \\ 0 & 0 & 1 & -\frac{1}{\Delta y_{12}} & 0 & \frac{1}{\Delta y_{12}} & 0 \\ 0 & 0 & 0 & \frac{\Delta y_{j2}}{\Delta y_{12}} & 0 & -\frac{\Delta y_{j1}}{\Delta y_{12}} & 0 \\ 0 & 0 & 0 & -\frac{\Delta x_{j1}}{\Delta y_{12}} & 1 & \frac{\Delta x_{j1}}{\Delta y_{12}} & 0 \\ 0 & 0 & 0 & -\frac{1}{\Delta y_{12}} & 0 & \frac{1}{\Delta y_{12}} & 0 \\ 0 & 0 & 0 & -\frac{\Delta x_{12}}{\Delta y_{12}} & -1 & \frac{\Delta x_{12}}{\Delta y_{12}} & 1 \end{bmatrix}$$

to obtain the reduced row echelon form

$$E_{ij12}O = \begin{bmatrix} \mathbf{I}_6 \\ \mathbf{0}_{1\times 6} \end{bmatrix} \tag{25}$$

This implies that two landmarks add three linearly independent rows to the observability matrix of graph G_n^2, which are linearly independent to the $3(n-1)$ existing rows. Therefore, the rank of the observability matrix for the RPMG G_n^l with $l = 2$ is $3n$. ■

Additional videos of simulation and experimental results related to bearing-only cooperative localization can be found in [22].

IV. Conclusion

In this paper we have shown that the observability properties of a system performing cooperative localization can be characterized by the properties of its relative position measurement graph (RPMG). Using graph theoretic properties and nonlinear observability theory, we have shown that for a connected proper RPMG G_n^0 without landmarks, the maximum rank of the observability matrix is $3(n-1)$. Furthermore, we have shown that to achieve full observability, all nodes in the graph must have a path to at least two different landmarks of known location.

References

[1] R. Kurazume and S. Hirose, "Study on cooperative positioning system: optimum moving strategies for CPS-III," in *Proc. IEEE International Conference on Robotics and Automation*, vol. 4, 16–20 May 1998, pp. 2896–2903.

[2] A. C. Sanderson, "A distributed algorithm for cooperative navigation among multiple mobile robots," *Advanced Robotics*, vol. 12, pp. 335–349, 1998.

[3] S. I. Roumeliotis and G. A. Bekey, "Collective localization: a distributed kalman filter approach to localization of groups of mobile robots," in *Proc. IEEE International Conference on Robotics and Automation ICRA '00*, vol. 3, 24–28 April 2000, pp. 2958–2965.

[4] J. Spletzer, A. Das, R. Fierro, C. Taylor, V. Kumar, and J. Ostrowski, "Cooperative localization and control for multi-robot manipulation," in *Proc. IEEE/RSJ International Conference on Intelligent Robots and Systems*, vol. 2, 2001, pp. 631–636.

[5] I. M. Rekleitis, G. Dudek, and E. E. Milios, "Multi-robot cooperative localization: a study of trade-offs between efficiency and accuracy," in *Proc. IEEE/RSJ International Conference on Intelligent Robots and System*, vol. 3, 30 Sept.–5 Oct. 2002, pp. 2690–2695.

[6] P. Nebot, D. Gomez, and E. Cervera, "Agents for cooperative heterogeneous mobile robotics: a case study," in *Proc. IEEE International Conference on Systems, Man and Cybernetics*, vol. 1, 5–8 Oct. 2003, pp. 557–562.

[7] A. Bahr, J. J. Leonard, and M. F. Fallon, "Cooperative localization for autonomous underwater vehicles," *International Journal of Robotics Research*, vol. 28 , Issue 6, pp. 714–728, 2009.

[8] A. Mourikis and S. Roumeliotis, "Analysis of positioning uncertainty in reconfigurable networks of heterogeneous mobile robots," in *Proc. IEEE International Conference on Robotics and Automation ICRA '04*, vol. 1, 2004, pp. 572–579.

[9] S. I. Roumeliotis and G. A. Bekey, "Distributed multirobot localization," *IEEE Transaction for Robotics and Autonomus Systems*, vol. 18, no. 5, pp. 781–795, 2002.

[10] A. Howard, M. J. Matark, and G. S. Sukhatme, "Localization for mobile robot teams using maximum likelihood estimation," in *Proc. IEEE/RSJ Int Intelligent Robots and Systems Conf*, vol. 1, 2002, pp. 434–439.

[11] D. Fox, W. Burgard, H. Kruppa, and S. Thrun, "A probabilistic approach to collaborative multi-robot localization," *Autonomous Robots*, vol. 8, pp. 325–344, 2000.

[12] E. D. Nerurkar, S. I. Roumeliotis, and A. Martinelli, "Distributed maximum a posteriori estimation for multi-robot cooperative localization," in *Proc. IEEE Int. Conf. Robotics and Automation ICRA '09*, 2009, pp. 1402–1409.

[13] A. Bicchi, D. Pratichizzo, A. Marigo, and A. Balestrino, "On the observability of mobile vehicles localization," in *IEEE Mediterranean Conference on Control and Systems*, 1998.

[14] G. Huang, A. Mourikis, and S. Roumeliotis, "Analysis and improvement of the consistency of extended kalman filter based SLAM," in *Proc. IEEE International Conference on Robotics and Automation ICRA 2008*, 2008, pp. 473–479.

[15] A. Martinelli and R. Siegwart, "Observability analysis for mobile robot localization," in *Proc. IEEE/RSJ International Conference on Intelligent Robots and Systems (IROS 2005)*, 2–6 Aug. 2005, pp. 1471–1476.

[16] M. Betke and L. Gurvits, "Mobile robot localization using landmarks," *IEEE Transaction for Robotics and Autonomus Systems*, vol. 13, no. 2, pp. 251–263, 1997.

[17] L. D. L. Perera, A. Melkumyan, and E. Nettleton, "On the linear and nonlinear observability analysis of the SLAM problem," in *Proc. IEEE Int. Conf. Mechatronics ICM 2009*, 2009, pp. 1–6.

[18] K. W. Lee, W. S. Wijesoma, and I. G. Javier, "On the observability and observability analysis of SLAM," in *Proc. IEEE/RSJ Int Intelligent Robots and Systems Conf*, 2006, pp. 3569–3574.

[19] A. Mourikis and S. Roumeliotis, "Performance analysis of multirobot cooperative localization," *IEEE Transaction for Robotics and Autonomus Systems*, vol. 22, no. 4, pp. 666–681, 2006.

[20] R. Hermann and A. Krener, "Nonlinear controllability and observability," *IEEE Transactions on Automatic Control*, vol. 22, no. 5, pp. 728–740, Oct 1977.

[21] G. Strang, *Introduction to Linear Algebra, 4th Edition.* Wellesley-Cambridge Press, 2009.

[22] *https://sites.google.com/site/rajnikantwiki/research/cooperative-localization*.